

Antithetic-dominated relics of the immature stage of the North-Armorican shear zone (Brittany, France)

Tine DEREZ¹, Sara VANDYCKE², Tom HAERINCK¹, Isaac BERWOUTS¹ and Manuel SINTUBIN¹

¹*Geodynamics & Geofluids Research Group, Department of Earth & Environmental Sciences, Katholieke Universiteit Leuven, Celestijnenlaan 200E, 3001 Leuven, Belgium*

²*Géologie Fondamentale et Appliquée, Faculté Polytechnique, Université de Mons, 9 rue de Houdain, 7000 Mons, Belgium*

ABSTRACT. The Palaeozoic North-Armorican shear zone (NASZ) (Brittany, France) is described as an E-W trending dextral, intracontinental shear zone. In the valley of the Queffleuth river, we outline a well-exposed zone of protocataclasite to cataclasite as the Queffleuth cataclastic zone (QCZ). Four morphological fault classes are defined in the QCZ based on the petrographic characteristics of the fault planes. The first fault class is clearly related to cataclasis, as the matrix/clast ratio increases and the clast size decreases towards the individual fault planes. The other three morphological classes cross-cut the cataclasite and are therefore considered to postdate cataclasis. A palaeostress analysis allowed to distinguish five distinct stress states, which are dominated by oblique to pure strike-slip N-S trending faults, that are oriented antithetic with respect to the overall trend of the NASZ. Both dextral and sinistral E-W kinematics are inferred for the QCZ. Because all morphological fault classes are identified in each of the stress states, dextral and sinistral kinematics must have occurred during and after cataclasis. Based on the kinematic similarities with the active South Iceland seismic zone, it is suggested that the defined stress states reflect local stress permutations during the early, immature stage of the NASZ.

KEYWORDS: Armorica, cataclasis, immature shear zone, palaeostress analysis, Queffleuth cataclastic zone, slip sense indicators, South Iceland seismic zone

RÉSUMÉ. Reliques antithétiques de la phase primitive du cisaillement Nord Armorica (Bretagne, France). La zone de cisaillement nord armoricain (NASZ) (Bretagne, France) orientée E-W et active au Paléozoïque est reconnue comme une zone de cisaillement dextre intracontinentale. La zone cataclasique de Queffleuth (QCZ) a été définie dans la vallée de Queffleuth au sein de la NASZ. La QCZ contient des protocataclasites à des cataclasites. Dans la QCZ, quatre classes morphologiques de failles ont pu être pétrographiquement définies. Perpendiculairement au plan de failles de la première classe, le pourcentage de matrice augmente tandis que le pourcentage de clastes diminue, en s'éloignant du plan de faille. De ce fait, cette classe est interprétée comme contemporaine des cataclasites. Les trois autres classes recoupent les cataclasites et sont ainsi datées post-cataclase. Il a été remarqué que l'orientation privilégiée des failles était N-S. Une analyse en termes de tenseurs de contrainte a permis d'identifier cinq événements cohérents. La prédominance de la direction N-S a été interprétée comme une expression antithétique par rapport au mouvement général de la NASZ. Il en résulte la récurrence de mouvements dextres et senestres de la QCZ pendant et après la phase de cataclase. Ainsi on propose une alternance de plusieurs tenseurs de contraintes pendant la phase primitive du cisaillement nord armoricain, comme dans la zone sismique du sud de l'Islande.

MOTS-CLÉS: Armorica, cataclasite, zone primitive du cisaillement, reconstruction des paléocontraintes, zone cataclasique de Queffleuth, marqueurs de cisaillement, zone sismique du sud de l'Islande

SAMENVATTING. Antithetische restanten van de primitieve fase van de Noord-Armoricaanse schuifvervormingszone (Bretagne, Frankrijk). De Palaeozoische Noord-Armoricaanse schuifvervormingszone (NASZ) (Bretagne, Frankrijk) wordt beschreven als een O-W georiënteerde dextrale intracontinentale schuifvervormingszone. In de vallei van de Queffleuth is een goed ontsloten zone met protocataclasis en cataclasis gedefinieerd als de Queffleuth cataclastische zone (QCZ). In de QCZ zijn vier morfologische breukklassen omlijnd op basis van de petrografische kenmerken van de breukvlakken. De eerste morfologische breukklasse is duidelijk gerelateerd met cataclase, doordat zowel de matrix/klast ratio stijgt, als de klastgrootte daalt naar de individuele breukvlakken toe. De breukvlakken van de andere drie morfologische breukklassen doorsnijden de cataclasis en worden daarom geïnterpreteerd als zijnde postcataclase. Met behulp van een palaeospanning analyse zijn vijf palaeospanning toestanden afgeleid van de meestal N-Z georiënteerde oblique tot laterale breuken. Deze N-Z breuken zijn antithetisch ten opzichte van de NASZ. Voor de QCZ zijn zowel dextrale als sinistrale O-W georiënteerde schuifvervorming afgeleid. Omdat alle palaeospanning toestanden gebaseerd zijn op een mengsel van breuken uit de verschillende morfologische breukklassen, hebben de dextrale en de sinistrale schuifvervorming plaatsgevonden tijdens en na cataclase. Er wordt voorgesteld dat de palaeospanning toestand lokaal wisselde tussen dextraal en sinistral tijdens een primitieve fase van de NASZ, zoals in de actieve Zuid-IJsland seismische zone.

SLEUTELWOORDEN: Armorica, cataclasis, primitieve schuifvervormingszone, palaeospanning analyse, Queffleuth cataclastische zone, schuifvervorming indicatoren, Zuid-IJsland seismische zone

1. Introduction

The North-Armorican shear zone (NASZ) is a Palaeozoic E-W oriented intracontinental shear zone (Cabanis *et al.*, 1981), which has been consistently described as a through-going dextral transcurrent shear zone that crosscuts the northern part of the Armorican massif (Fig. 1). Due to the poor degree of exposure, the temporal, spatial and kinematic relationship of the scattered observations of cataclasite and mylonite is rather challenging (Fig. 1). A unique opportunity to study the kinematics of the NASZ is present in the valley of the Queffleuth, south of Morlaix, where a road cut, oriented perpendicular to the map trace of the NASZ, provides excellent exposure of the fault rocks that are considered to materialize the NASZ (Cabanis *et al.*, 1981) (Fig. 2). The road-cut section exposes a N-S oriented, 80m wide zone

containing protocataclasite to cataclasite, which we define as the *Queffleuth cataclastic zone* (QCZ). This study reconstructs the kinematic evolution of the QCZ, based on a field study of the brittle deformation features, a microfabric study of the fault rocks and a palaeostress inversion analysis. Furthermore, this study serves as a test case of the applicability of the palaeostress inversion method of Angelier (1990) on brittle-ductile shear zones formed by cataclastic flow, as previously exemplified in studies of Wilson *et al.* (2006) and Srivastava *et al.* (1995).

2. Geological setting

The geological subsurface of Brittany exposes a part of Armorica, a Gondwana-derived microcontinent that has been incorporated in the Pan-European Variscan orogenic belt between 440 and

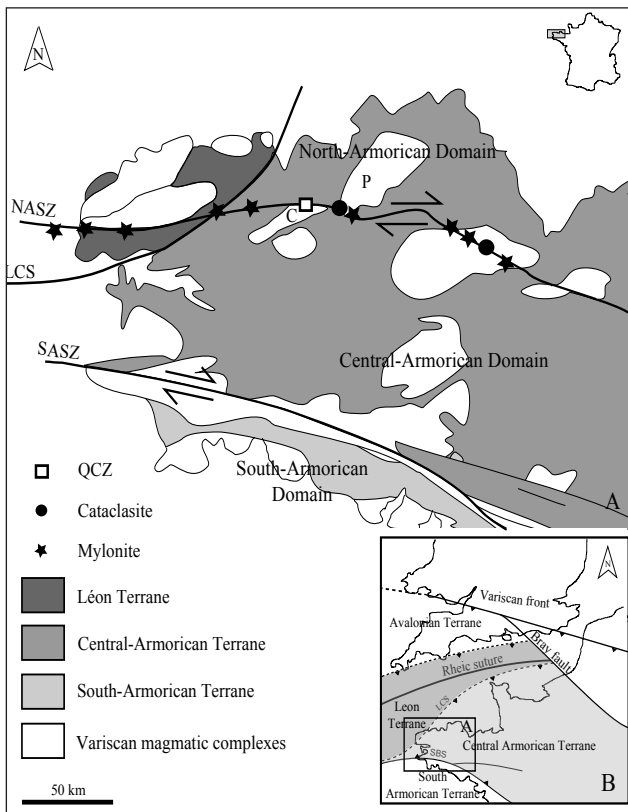


Figure 1. (A) Tectonostratigraphic map of western Brittany with indications of the outcrops of mylonite (black stars) and cataclasite (black circles) along the trace of the NASZ as described in literature. (B) Variscan terrane map of northwestern Europe. C: Commana granite, LCS: Le Conquet Suture, NASZ: North-Armorican shear zone, P: Plouaret granite, QCZ: Queffleuth cataclastic zone, SASZ: South-Armorican shear zone, SBS: South-Brittany Suture (after Matte, 2001; Gumiaux et al., 2004; Faure et al., 2005).

290 Ma (Faure et al., 2005; Le Corre et al., 1991; Matte, 2001). Armorica is subdivided into several tectonostratigraphic domains (Fig. 1). The NASZ forms the boundary between the North-Armorican and the Central-Armorican domain, and crosscuts the Léon domain to the west (Faure et al, 2008). The shear sense of the NASZ is suggested to have been dextral, based on the map-based, apparent displacement of the magmatic complexes (Fig. 1) on the one hand and S-C mylonitic fabrics on the other hand (Chauris, 1969; Chauris & Garreau, 1975; Ballèvre et al., 2009; Berwouts, 2011; Castaing et al., 1987; Darboux, 1991; Faure et al., 2005, 2008; Gapais & Cobbold, 1987; Garreau, 1983; Goré & Le Corre, 1987; Le Corre et al., 1991; Watts & Williams, 1979).

The dextral displacement along the NASZ is estimated to be 10 to 20 km, primarily based on the present-day map geometry of the late-Variscan magmatic complexes along the NASZ trace (Chauris, 1969; Garreau, 1983; Goré & Le Corre, 1987; Watts & Williams, 1979). Gumiaux et al. (2004) interpret the NASZ and the South-Armorican shear zone as the boundary faults of a large strike-slip shear belt, the ‘Central Brittany shear zone’, active between 355 and 300 Ma.

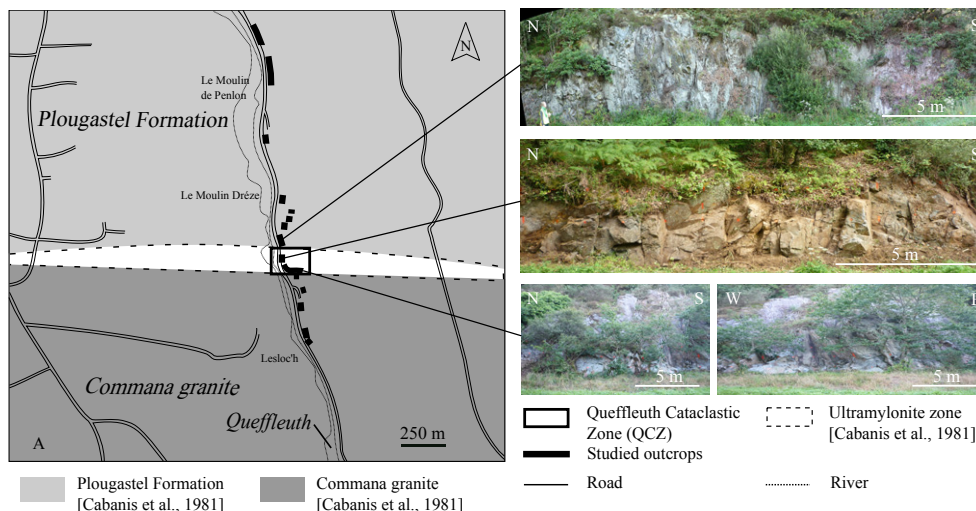
Most authors agree that the NASZ was dominantly active during the late stages of the Variscan orogeny (Chauris, 1969; Faure et al., 2010; Garreau, 1983; Roach, 1980). According to Berthé et al. (1979), the shear zone was active during the Middle to Late Carboniferous, postdating a contraction-dominated tectonic stage, called the ‘Bretonian event’ (late Devonian-early Carboniferous) (see Sintubin et al., 2008 and references therein). The latter time constraint is corroborated in the wider Queffleuth area by the presence of veins in the Plougastel Formation, interpreted to be linked to the activity of the NASZ, that crosscut a slaty cleavage that is considered to reflect the Bretonian deformation event (Berwouts, 2011). The undeformed Bas-Léon granite (292 ± 9 Ma) and the Belle-Isle-en-Terre microgranite (292 ± 13 Ma) define the minimum age of NASZ activity (Berwouts, 2011 and references therein). Some authors have moreover suggested that the NASZ is a reactivated Neoproterozoic structure (Strachan et al., 1989; Watts & Williams, 1979).

According to the geological map (Cabanis et al., 1981), an E-W oriented ultramylonitic zone, materializing the NASZ in the study area, forms the contact between the Plougastel Formation, a Silurian-Devonian (420-416 Ma) multilayer sequence of metapelite and quartzitic siltstones, to the north and the Commana granite, a porphyritic monzogranite, to the south (Fig. 2). The Commana granite, is interpreted as part of the Commana-Plouaret complex, dated at 329 ± 5 Ma (Carron et al., 1994), that is subsequently dextrally displaced by the NASZ (Carron et al., 1994).

3. Methodology

The structure and lithology of the QCZ, was studied in 16 individual outcrops, along the near continuous road-cut section in the valley of the Queffleuth river (Fig. 2). For the purpose of the palaeostress analysis, special attention was paid to fault planes and slip markers (148 fault slip data collected). The exposed surface area (cm^2), the orientation of each individual fault plane, the orientation of each linear slip marker, and if possible its slip sense, were measured. A confidence level was attributed to each slip sense indicator. In a number of cases, the amount of displacement could be determined in thin section, only for small-scale displacements. Linear slip markers, such as slickenlines and slickenfibres, were measured as the pitch in the plane. Based solely on their macroscopic appearance, faults were categorized into four morphological classes, independent of their orientation and/or slip sense (Fig. 3). This macroscopic separation aimed at verifying whether faults from an identical morphological class are

Figure 2. (A) Schematic map of the study area. According to Cabanis et al. (1981) an E-W oriented ultramylonite lenticular body (white zone bordered by a dashed line) separating the Plougastel Formation (to the north) and the Commana granite (to the south), is exposed along the section studied. All studied outcrops are indicated with black rectangles and some are illustrated with an overview picture.



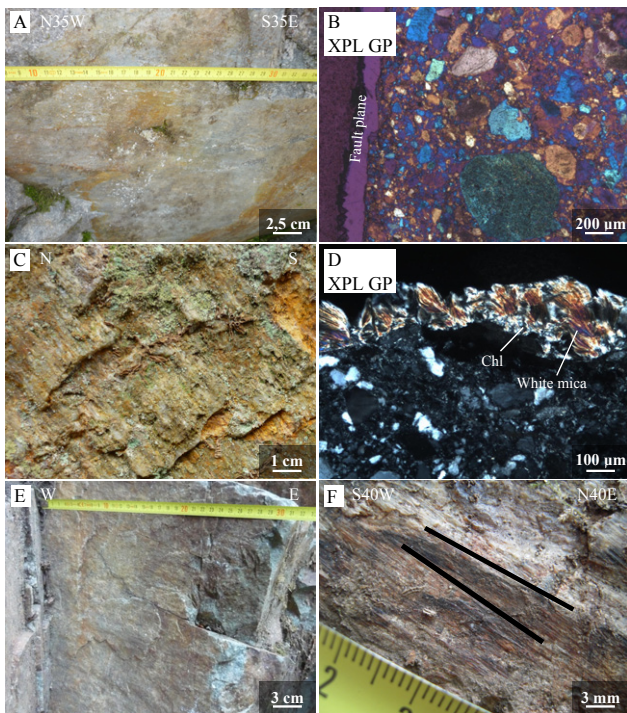


Figure 3. Fault classes in the QCZ. (A) Fault plane of class A. (B) Optical microscope photograph of a cross-section through a fault plane of class A. (C) Fault plane of class B with extensive slickenfibres. (D) Optical microscope photograph of a cross-section through a fault plane of class B. (E) Fault plane with slickenlines, of class C. (F) Fault plane of class D. Two slickenfibres are marked with black lines. Chl: Chlorite, GP: gypsum plate, XPL: cross-polarised light.

indicative of similar tectonometamorphic formation conditions (cf. Delvaux & Sperner, 2003).

The palaeostress analysis was executed with the software package TENSOR designed by Angelier (1990). The theoretical background of the method is well described by different authors (Angelier, 1979; Etchecopar et al., 1981; Lacombe, 2012). A semi-automatic, iterative procedure groups faults in their respective stress states of possible (re)activation. When the coherence of the calculated stress state is less than 100%, the quality parameters of the fault planes is evaluated. Each data point represents one single fault plane.

When the pitch of the linear slip markers is between 10° and 80° , the slip is considered oblique. True oblique slip can occur on reactivated faults or activated planes of weakness, while apparent oblique slip can be caused by block tilting of a former, newly formed fault (Angelier, 1990). Due to the basic assumptions of the paleostress inversion method (Angelier, 1990), the palaeostress orientation deduced from reactivated faults or activated planes of weakness will not have an oblique component. In contrary, tilting of faults and a small spatial dispersion of the faults will cause the stress state to reflect an oblique component (Angelier, 1994).

Thirty samples were collected for the petrofabric analysis. By means of optical microscopy and image analysis, fault rocks in the QCZ were classified, following the classification scheme of Scholtz (2003). Digital image analysis on thin sections, performed with Image-Pro Plus (Version 5.0), enabled to determine the matrix/clast ratio of the fault rocks. However, classifying fault rocks is an ambiguous procedure, primarily because the result depends on the scale of observation and the chosen classification scheme. The magnification, used during microscopy, determines the minimum size of a domain that can be identified as a clast. Moreover, most of the classification schemes used do not prescribe the magnification at which a clast has to be identified. To compare fault rocks, an extensive description on different scales is therefore imperative. Shear sense indicators in mutually perpendicular thin sections indicate the kinematics on a microscale.

4. Petrography

4.1. Queffleuth Cataclastic Zone

The rocks in the northern part of the QCZ consist of angular clasts of feldspar and quartz embedded in a grey, fine-grained matrix. More to the south, lenses of fractured granite are incorporated in a matrix-dominated rock with clasts of feldspar and quartz. On the microscale, the matrix-dominated rock consists of crosscutting bands with a uniform grain size, showing uniform interference colours upon inserting a gypsum wedge. Throughout the QCZ, the cataclasite consists of 22 to 68% matrix. Because no spaced foliation, composed of alternating layers and lenses with different mineral composition, is present, the rocks are classified as protocataclasite to cataclasite (Scholtz, 2003). From north to south in the QCZ, the degree of cataclasis decreases.

The small grain size makes it impossible to determine the composition of the matrix using optical microscopy. It is however, likely that the matrix consists predominantly of quartz and feldspar, the same mineralogy as the clasts. Chlorite, white mica and opaque minerals are present in subsidiary amounts in the matrix. White mica coats individual clasts of quartz and feldspar, and is also present in veins that are crosscut by matrix-dominated bands (Plate 1A). Epidote is an accessory mineral in the matrix.

Intercrystalline deformation mechanisms, e.g. kinked mica (Plate 1B), bookshelf microfracturing (Plate 1C to 1F), δ -type winged mantled clasts (Plate 1G) and fragmented and displaced clasts (Plate 1H to 1M), serve as shear sense indicator. The microstructures indicate both sinistral and dextral shear senses with displacements in the order of $100\ \mu\text{m}$. Intracrystalline deformation structures, e.g. bent twins in plagioclase (Plate 1N), and crystal-plastic deformation as bulging and subgrain rotation recrystallisation in quartz grains (Plate 1O), are also present.

4.2. Plougastel Formation

North of the QCZ, rocks of the Plougastel Formation, a metasedimentary multilayer sequence of alternating quartzitic siltstone and metapelite, are well exposed (Fig. 2). The metapelites contain randomly oriented muscovite and andalusite porphyroblasts. The lack of any strain shadows indicates that porphyroblastesis postdates cleavage development. A wavy disjunctive cleavage is present in the quartzitic siltstone; a crenulation cleavage in the metapelite. Cleavage has a consistent attitude of $\sim 180/80$. Berwouts (2011) shows that the cleavage resulted from the contraction-dominated Bretonnian event (late Devonian-early Carboniferous). Small faults ($\sim 325/90$), with sinistral kinematics, strongly affect bedding and cleavage in the outcrop directly north of the QCZ (Fig 2a). Similar small faults have not been observed further to the north.

4.3. Commana granite

The Commana granite is a phanero-, holocrystalline monzogranite with a porphyritic microstructure. The main minerals are feldspar (50%), with plagioclase slightly more dominant than alkali-feldspar, and quartz (35%). Deformation twins are present in plagioclase, while bulging and subgrain rotation recrystallisation are recognised in quartz. Biotite (10%) is an important subsidiary mineral, often replaced by chlorite along crystallographic basal planes. Chlorite and white mica are accessory minerals. Directly south of the QCZ, the monzogranite is fractured and contains several small zones of cataclasite. No mylonitic foliation is present. The cataclasite disappears 50m south of the QCZ, except for a 20cm wide zone, 500m south of the QCZ, containing protocataclasite with a 46% bright grey, fine-grained matrix, and quartz/feldspar clasts. Four km south of the QCZ, indicators of any major deformation are no longer present.

4.4. Commana granite as the cataclasite protolith

The Commana granite is the most likely protolith of the quartz- and feldspar-rich fault rocks, despite some mineralogical differences. Biotite for example, is abundant in the Commana granite, but is absent in the cataclasite. An alteration of biotite to chlorite is suggested, although it may also be disseminated

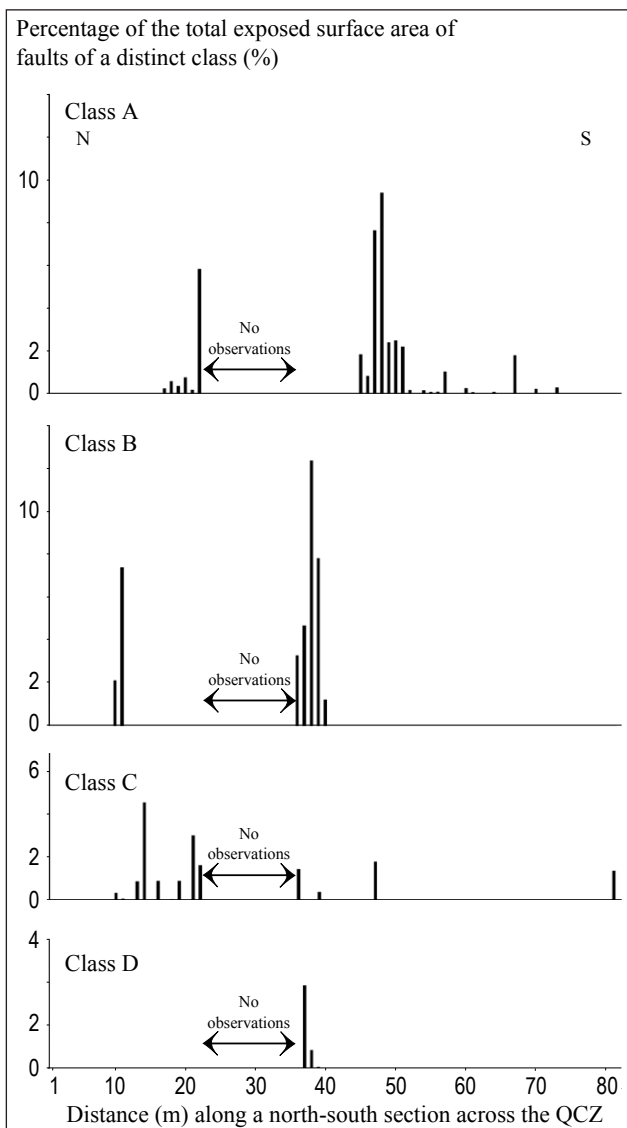


Figure 4. Distribution of the morphological fault classes in the QCZ, shown as stacked column diagrams of the percentage of the total exposed surface area of measured fault planes per class, along a north-south section across the QCZ (m). Between meter 24 and meter 34 the QCZ is not exposed.

in the fine-grained matrix. Additionally, epidote is only present in the cataclasite, not in the granite. It is suggested that the epidote was formed as a secondary mineral due to hydrothermal alteration (saussuritisation) of plagioclase (e.g. Deer et al., 1992). The white mica in the matrix originates most likely from cataclasis of the felsic igneous protolith, as an alteration product of feldspar. The white mica in seams around individual clasts and within veins has most probably been precipitated from a fluid. Precipitation of quartz during cataclasis may explain the compact,

homogeneous and competent nature of the fault rocks. Berwouts (2011) demonstrated that significant fluid flow is concentrated in antithetic cataclastic bodies cross-cutting the NASZ. Along the NASZ itself, no direct indications for significant fluid flow are found.

5. Fault plane characterisation

Four morphological fault classes were identified in the field. *Class A* comprises 69 smooth to wavy fault planes with a bright blue to grey colour, and marked by slickenlines (Fig. 3A). In cross section on the microscale, the matrix/clast ratio increases, while the clast size decreases towards the fault plane (Fig. 3B). These petrographic characteristics indicate that the fault planes of class A can be directly related to cataclasis.

Class B includes 37 wavy surfaces with extensive slickenfibres (Fig. 3C). The fibre-sheet imbrication is a good slip sense indicator, with a high degree of certainty. In thin section, a layered coating of chlorite and white mica is visible on the fault planes. The bottom layer of the coating consists of fine-grained white mica. On top of this layer, radiating, fibrous crystals of white mica and chlorite are present (Fig. 3D). The white mica crystals are inclined with respect to the contact with the matrix-dominated rock. Some quartz crystals are embedded in the coating. The contact of the coating with the matrix-dominated rock is irregular and no decrease in matrix/clast ratio is observed towards the fault plane. These observations indicate that class B fault planes are not related to cataclasis.

Class C contains 34 smooth surfaces on which slickenlines are difficult to recognise (Fig. 3E). The 8 wavy surfaces of *class D* reflect a mineral precipitation with two superposed slickenfibres orientations (Fig. 3F). Most often the oldest slickenfibres has a large wavelength with a small pitch, while the younger slickenfibres has a smaller wavelength with a larger pitch. The average angular difference between the pitch of both linear slip markers is 14° . The fibre-sheet imbrication is less pronounced than for class B, although the slip sense is distinguishable with a fairly high degree of certainty. Because of sampling difficulties, the fault planes of classes C and D were not investigated microscopically.

The spatial distribution of the fault classes is shown in Fig. 4 as the ratio of the percentage of the total exposed surface area of each class, to the total exposed surface area of all measured fault planes. Whereas faults of class A are markedly more present in the southern half of the section, the other classes are more concentrated in the northern part.

Fault slip data indicate a strike-slip movement. Faults are generally oriented NNE-SSW to NNW-SSE and E-W. Most of the linear slip markers plunge to the south (Fig. 5). The plunge of the linear slip markers of class C falls primarily to the west and to a lesser extent to the south. The pitch of the linear slip markers is generally between 0° and 40° , which means that slip dominantly reflects pure strike-slip to oblique slip (Angelier, 1994). While class C contains in particular E-W trending fault planes, showing a more diffuse orientation distribution than the other classes (Fig. 5C), the approximate N-S orientation of the majority of the fault planes of classes A, B and D is striking (Fig. 5A, 5B and 5D).

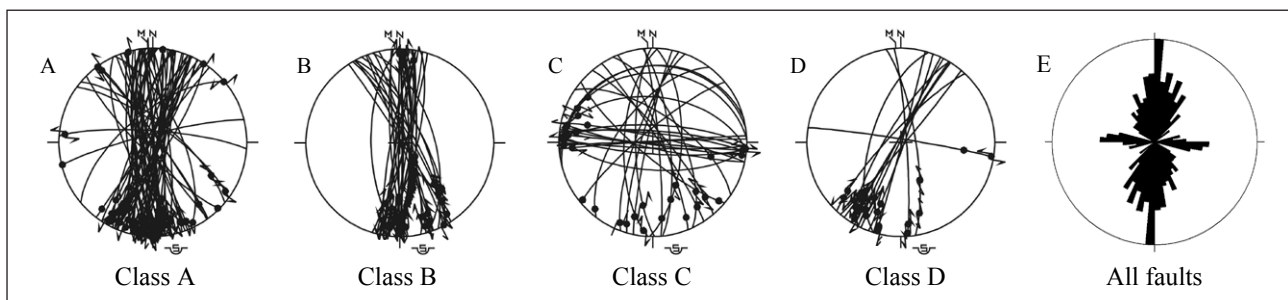


Figure 5. Fault orientation per morphological fault class in lower-hemisphere equal-area projections. (A) class A, (B) class B, (C) class C and (D) class D. The linear slip markers are indicated as black dots, the arrows indicate the slip sense. N: geographic north, M: magnetic north. (E) Rose diagram of all fault planes measured in the QCZ (N=148).

Stress state	N	Trend of σ_1 (°)	Dip of σ_1 (°)	Trend of σ_2 (°)	Dip of σ_2 (°)	Trend of σ_3 (°)	Dip of σ_3 (°)	Shape ratio ϕ	COH (%)	RUP (%)	OBL (°)	ANG (°)
Ideal									100	<50	<45	<45
1	9	279	4	14	53	186	37	0,3	100	18	22	6
2	11	173	19	26	67	268	11	0,4	100	7	9	3
3	45	315	9	130	81	225	1	0,8	100	12	14	6
4	33	139	10	47	13	264	74	0,4	100	37	20	13
5	27	52	12	247	77	142	3	0,8	100	29	23	12

Table 1. Palaeostress analysis in the QCZ. The successive columns show the calculated stress state, N: the number of faults, the orientation of σ_1 , σ_2 and σ_3 , ϕ : $((\sigma_2 - \sigma_3) / (\sigma_1 - \sigma_3))$, COH: coherence percentage, RUP: ratio epsilon or the percentage of convenience, OBL: lateral variation between the expected orientation of the slip markers, related to the calculated stress state, and the observed slip markers, ANG: vertical variation between the expected orientation of the slip markers, related to the calculated stress state, and the observed slip markers. The ideal values for the quality parameters are suggested by Angelier (1990).

6. Palaeostress analysis

The palaeostress inversion technique of Angelier (1994) is recognised as a useful technique to determine the principal stress axes based on faults related to cataclasis (Wilson et al., 2006; Srivastava et al., 1995). During the iterative process of palaeostress analysis, the orientation of the principal stress axes remained relatively constant, as confirmed by satisfying quality parameters. In contrary, the relative magnitude of the principal stresses (the stress ratio $\phi = (\sigma_2 - \sigma_3) / (\sigma_1 - \sigma_3)$) was highly variable, which can be caused by a limited spatial dispersion of the faults. However, this did not obstruct a more or less accurate determination of the stress states (Lacombe, 2012). Further, the application of palaeostress analysis is only valid under circumstances of coaxial deformation (Wilson et al., 2006). No indications for non-coaxial deformation were observed in the case of the QCZ, as the cataclastic zone has a homogeneous appearance and the orientation of the oldest class A faults is similar to that of the later fault classes.

Five distinct stress states were determined (see Table 1 and Fig. 6). Stress states 1 and 2 have a similarly oriented stress field, with the intermediate principal stress axis σ_2 having a small oblique component, while their principal stress axes σ_1 and σ_3 are E-W and N-S oriented, respectively. Stress states 3, 4 and 5 are based on faults with a general N-S and E-W orientation. One principal stress axis is approximately vertical and two other axes are subhorizontal and NE-SW and NW-SE striking.

None of the four morphological fault classes can be attributed to a single stress state (Fig. 7). Therefore, the spatial distribution of the different faults classes within the QCZ (Fig. 4) can be explained by a spatial variability in rock properties.

Based on the microscopic observations, the faults of class A are related to cataclasis. They are interpreted to be the main cataclasite-forming faults. Although the faults of classes C and D were not studied on the microscale, it is thought that they crosscut the cataclasite as do the faults of class B, which are effectively inferred to postdate cataclasis.

7. Stress state evolution

The distribution of the different fault classes in the calculated stress states can be used to constrain relative timing of the different stress states. Stress states 1 and 2 are not compatible with the class A faults, indicating that both stress states postdate cataclasis. On the contrary, the other stress states 3 to 5 are partly based on class A faults, suggesting fault activity related to these stress states was largely contemporaneous to cataclastic flow. Only the youngest stress states 1 and 2 show an oblique component. The absence of this oblique component in the older stress states 3 to 5 precludes block tilting. The small oblique component in stress states 1 and 2 is therefore probably related to the small spatial dispersion of the faults in question (Angelier, 1994), i.e. an artefact due to scarcity of data.

Stress state 3 indicates dextral kinematics, while stress state 5 indicates sinistral kinematics, both for an E-W trending shear zone (Fig. 6). In the Riedel framework (Riedel, 1928; Tchalenko, 1970), the N-S oriented, sinistral faults belonging to stress state 3 are interpreted as antithetic R' faults within an overall dextral shear zone with a N75W strike. Hence, the approximately E-W oriented, dextral fault belonging to stress state 3 can be

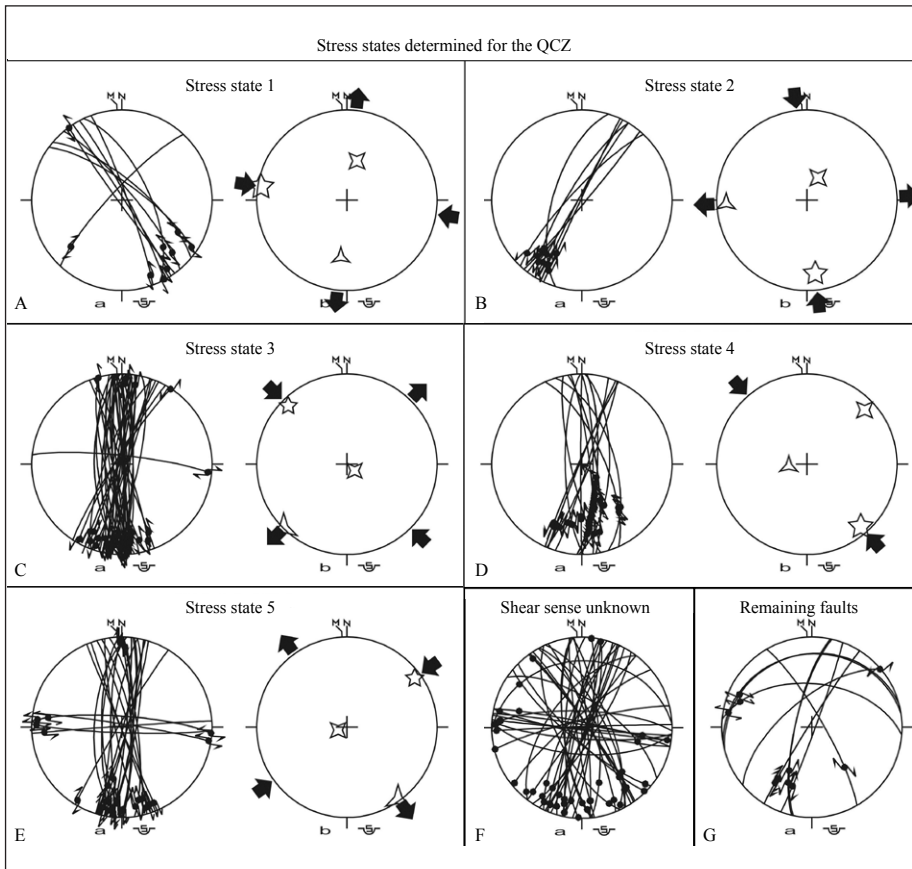


Figure 6. Palaeostress analysis in the QCZ. (A) Strike-slip regime with a compression E-W/extension N-S (stress state 1), (B) strike-slip regime with a compression N-S/extension E-W (stress state 2), (C) strike-slip regime with a compression NW-SE/extension NE-SW (stress state 3), (D) Compression NW-SE with oblique strike-slip faults (stress state 4), (E) strike-slip regime with a compression NE-SW/extension NW/SE (stress state 5). (F) Fault planes with an unknown slip sense. (G) Fault planes that do not match the determined stress states. The diagrams *a* on the left, show lower-hemisphere equal-area projection of fault planes (great circles). The slip markers are indicated as black dots, the arrows indicate the slip sense. The diagrams *b* on the right, are lower-hemisphere equal-area projections, containing the computed principal stress axes σ_1 , σ_2 and σ_3 , shown as 5-, 4- and 3-branched stars, respectively. The large black arrows indicate the directions of horizontal compression and extension. N: geographic north, M: magnetic north. The numerical results of the palaeostress analysis are shown in Table 1.

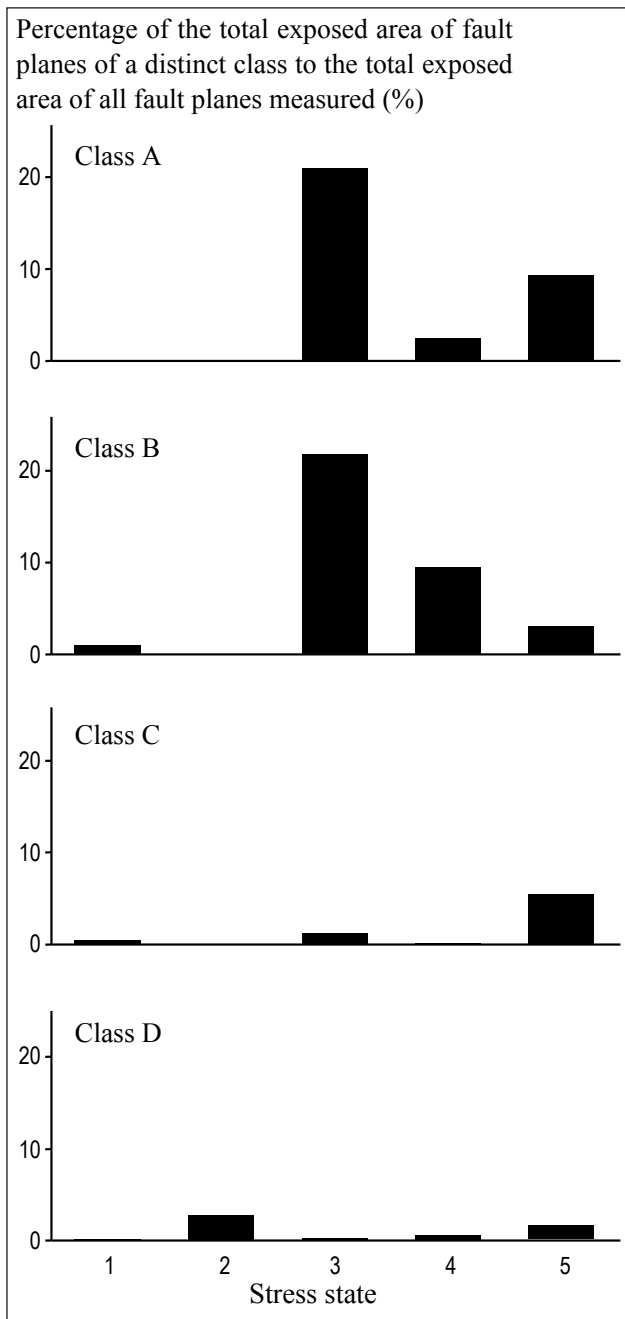
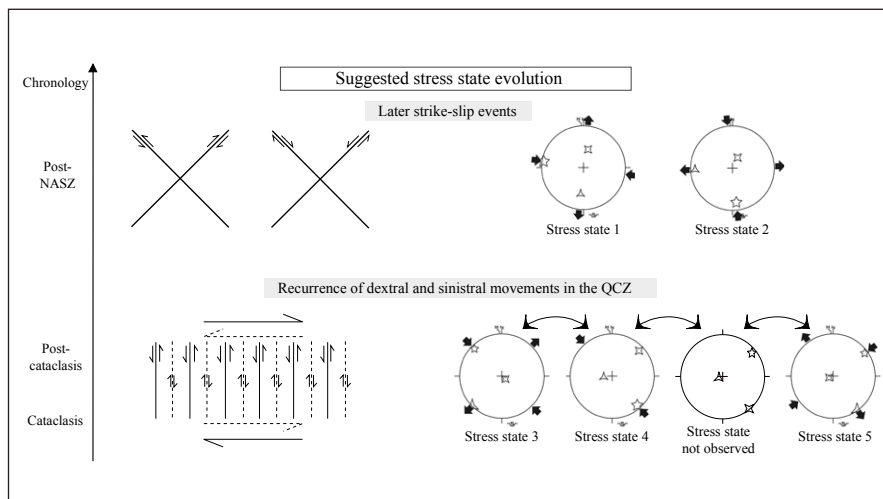


Figure 7. Distribution of faults of the four distinct morphological classes with respect to the different stress states. The stacked column diagram shows the amount of faults, as the ratio of the total exposed area of fault planes of a distinct class to the total exposed area of all fault planes measured (%), per stress state.

Figure 8. Stress state evolution in the QCZ. Diagram illustrating a permutation of dextral (full arrows) (stress states 3) and sinistral E-W trending kinematics (dashed arrows) (stress state 5), due to the inversion or rotation of the principal stress axes during and after cataclasis. Subsequently, the area is crosscut by oblique strike-slip faults (stress states 1 and 2). The plots are lower-hemisphere equal-area projections and contain the computed principal stress axes σ_1 , σ_2 and σ_3 , shown as 5-, 4- and 3-branched stars, respectively. The large black arrows indicate the directions of maximum and minimum horizontal stress. N: geographic north, M: magnetic north.



interpreted as a synthetic P fault. The N-S oriented, dextral fault planes belonging to stress state 5 are interpreted as antithetic R' faults within an overall sinistral shear zone with N75E strike. The E-W oriented, sinistral faults belonging to stress state 5 represent synthetic P faults. It is striking that most faults are antithetic (R') with respect to the overall trend of the shear zone, and that synthetic R faults are completely absent.

Stress state 4 is the only compressive stress state derived. The mostly N-S oriented faults on which stress state 4 is based, are subvertical and have slip markers with a pitch varying between 20° and 40°. Because of the oblique slip and the approximately vertical orientation of the minimum principal stress axis σ_3 , it is suggested that these faults represent slip reactivation of faults that have been formed in stress states 3 or 5. Stress state 4 is interpreted as an intermediate stress state necessary to permute from dextral (stress state 3) to sinistral (stress state 5) kinematics and vice versa (Fig. 8). The equivalent intermediate stress state, necessary for the considered stress permutation (Fig. 8), has not been observed. The presence of the intermediate stress state 4 is moreover seen as an argument to exclude a stress permutation through an isotropic stress state. Van Noten et al. (2011, 2012) also suggested that an evolution through an isotropic stress state is improbable.

8. Discussion and conclusion

The fault rocks in the QCZ have been demonstrated to be non-foliated protocataclasis to cataclasis, according to the classification scheme of Scholz (2003). This observation refutes the presence of an ultramylonite, as indicated on the geological map of Cabanis et al. (1981). The Commana granite is considered to be the most likely protolith of the cataclastic rock. The granite shows an increased fracturing in the vicinity of the QCZ, corroborating the progressive development of the cataclastic body within the Commana granite. The influence of the fault activity in the QCZ on the Plougastel Formation is, on the other hand, very limited, as the small sinistral faults (325/90), observed just north of the QCZ, are not compatible with one of the stress states that are linked to the strike-slip fault activity within the QCZ (stress states 3, 4 and 5). They rather relate to stress state 2 and should thus be regarded as younger than the QCZ activity. Therefore our study cannot be conclusive on the nature of the contact (intrusive or tectonic) between the Commana granite and the Plougastel Formation. Carron et al. (1994) state that this is a tectonic contact, i.e. the NASZ, as the Commana granite is supposed to be part of the Commana-Plouaret complex that is dextrally displaced along the NASZ. The fluid-assisted alteration of the cataclasis, moreover, suggests that the QCZ should rather be considered a ~N-S oriented, antithetic cataclastic body cross-cutting the NASZ (cf. Berwouts 2011). This interpretation is contrary to the E-W oriented trace of the ultramylonitic body as shown on the map of Cabanis et al. (1981) (Fig. 2).

The NASZ strike-slip regime has dominantly been regarded as being dextral (Chauris, 1969; Chauris & Garreau, 1975; Ballèvre et al., 2009; Berwouts, 2011; Castaing et al., 1987; Darboux,

1991; Faure et al., 2005, 2008; Gapais & Cobbold, 1987; Garreau, 1983; Goré & Le Corre, 1987; Le Corre et al., 1991; Watts & Williams, 1979). This study, however, indicates a recurrence of both dextral and sinistral kinematics in the QCZ. Berwouts (2011) also identified sinistral kinematics along the NASZ in the Elorn area, situated 7 km to the west of the Queffleuth valley, primarily based on the cleavage patterns in the proximity of the NASZ. For the Central-Armorican Domain sinistral kinematics has, moreover, been suggested by Darboux (1991) and Badham (1982) during early Variscan deformation.

The faults measured are dominantly antithetic with respect to the overall E-W oriented NASZ. A similar dominance of antithetic fault activity is found in currently active, immature shear zones (Bergerat & Angelier, 2008; Kilb & Rubin, 2002; Kim et al., 2003). According to Bergerat & Angelier (2008) an immature shear zone is typified by a rather straightforward stress pattern, related to a dominance of Riedel-type antithetic faults within a rather diffuse shear zone. When becoming more mature, the shear zone becomes through-going, showing a complex stress pattern. A similar dominance of antithetic faults in the early stages of shear zone activity is described by Kim et al. (2003, 2004) in damage zones of strike-slip faults at Gozo Island, Malta. These antithetic faults can be activated as tip- and linking damage zone structures, which afterwards evolve into wall damage zone structures as the main fault propagates. The antithetic faults in the wall damage zone structure subsequently rotate towards a trend perpendicular to the general displacement direction (Kim et al., 2003).

The inferred stress permutations between dextral and sinistral kinematics for the QCZ are also observed for the currently active, immature, antithetic-dominated, E-W oriented South Iceland seismic zone (Bergerat & Angelier, 2008). Bergerat & Angelier (2008) inferred four stress states. Two stress states are characterised by a NW-SE direction of extension, the other two have a NE-SW direction of extension. The stress states are thought to have alternated and probably oscillated in time reflecting the permutation between minor dextral strike-slip kinematics and main sinistral transform kinematics (Bergerat & Angelier, 2008). In the QCZ, no time constraints are available on the alternation between sinistral and dextral kinematics, though interestingly, focal mechanisms of earthquakes along the South Iceland seismic zone show that such a switch can even take place within a time span of 13 years (Bergerat & Angelier, 2008). Our findings suggest that the cataclasite of the QCZ preserved antithetic-dominated relics of both sinistral and dextral strike-slip kinematics along the NASZ. In analogy to the South Iceland seismic zone (Bergerat & Angelier, 2008), we therefore propose that the QCZ, is a fossil relic of the immature stage of the NASZ.

9. Acknowledgments

The research of T. Haerinch is financially supported by research grant G.0376.09N of the FWO-Vlaanderen, Belgium. S. Vandycke is Research Associate at the FNRS (National Research Foundation of Belgium). This research is financially supported by research Grant OT/11/038 of the Onderzoeksfonds KU Leuven.

10. References

- Angelier, J., 1979. Determination of the mean principal directions of stresses for a given fault population. *Tectonophysics*, 56, 17-26.
- Angelier, J., 1990. Inversion of field data in fault tectonics to obtain the regional stress – III. A new rapid direct inversion method by analytical means. *Geophysical Journal International*, 103, 363-376.
- Angelier, J., 1994. Fault slip analysis and paleostress reconstruction. In: Hancock, P. L., *Continental Deformation*. Pergamon Press, 53-101.
- Autran, A. & Cogné, J., 1980. La zone interne de l'orogène Varisque dans l'ouest de la France et sa place dans le développement de la chaîne Hercynienne. In: Cogné, J., & Slansky, M. (eds), *Géologie de l'Europe du Précambrien aux bassins sédimentaires post-Hercyniens*. 26^e Congr. Géol. Intern., Coll C6, Paris. Mém. BRGM, 108, 90-111.
- Badham, J.P.N., 1982. Strike-slip orogens: an explanation for the Hercynides. *Journal of the Geological Society, London*, 139, 493-504.
- Bergerat, F. & Angelier, J., 2008. Immature and mature transform zones near a hot spot: The South Iceland Seismic Zone and the Tjörnes Fracture Zone (Iceland). *Tectonophysics*, 447, 142-154.
- Berthe, D., Choukroune, P. & Gapais, D., 1979. Orientations préférentielles du quartz et orthogneissification progressive en régime cisailant: l'exemple du cisaillement sud-armoricain. *Bulletin de Minéralogie*, 102, 265-272.
- Berwouts, I., 2011. Reconstruction of fluid system evolution in a wrench tectonic setting. Implications for the geodynamic history of Central Armorica, Brittany, France. Ph.D. thesis, Aardkundige Mededelingen, volume 26. Leuven University Press, Leuven, 253.
- Brun, J.P. & Burg, J.P., 1982. Combined thrusting and wrenching in the Ibero-Armoricain arc: a corner effect during continental collision. *Earth and Planetary Science Letters*, 61, 319-332.
- Burg, J.P., Bale, P., Brun, J.P. & Girardeau, J., 1987. Stretching lineation and transport direction in the Ibero-Armoricain arc during the siluro-devonian collision. *Geodynamica Acta*, Paris, 1, 1, 71-87.
- Cabanis, B. et al., 1981. Carte géologique de la France a 1/50 000, feuille Morlaix (240). Bureau de Recherches Géologiques et Minières, Orléans.
- Carron, J.-P., Le Guen de Kerneizon, M. & Nachit, H., 1994. Variscan Granites from Brittany. In: Keppie, ED. J. *Pre-Mesozoic Geology in France and related areas*. Springer-Verlag Berlin Heidelberg, 231-237.
- Castaing, C., Rolet, J., Chevremont, P., Le Calvez, J.Y. & Thonon, P., 1987. La région de Huelgoat (Finistère central) dans le contexte géodynamique armoricain. *Géologie de la France*, 1, 23-36.
- Chauris, L., 1969. Sur un important accident structural dans le Nord-Ouest de l'Armorique. *Comptes Rendus de l'Académie des Sciences, Paris*, 2859-2861.
- Chauris, L. & Garreau, J., 1975. Les relations du granite de Guimiliau avec le Paléozoïque de la rade de Brest et du bassin de Morlaix (Massif Armoricain). *C. R. Acad. Sc. Paris*, 280, 251-254.
- Darboux, J.-R., 1991. Evolution tectonosédimentaire et structuration synmétamorphe des zones externes du segment hercynien ouest-européen: Le Modèle du Domaine Centre Armoricain occidental. Thèse d'état, Université de Bretagne Occidentale, Brest, 267.
- Deer, W. A., Howie, R.A. & Zussman, J., 1992. *An Introduction to the Rock-Forming minerals*. Longman Group UK Limited, 696.
- Delvaux, D. & Sperner, B., 2003. New aspects of tectonic stress inversion with reference to the TENSOR program. *Geological Society, London, Special publications*, 212, 75-100.
- Etchecopar, A., Vasseur, G. & Daignieres, M., 1981. An inverse problem in microtectonics for the determination of stress tensors from fault striation analysis. *Journal of Structural Geology*, 3, 51-65.
- Faure, M., Mézeme, E.B., Duguet, M., Cartier, C. & Talbot, J.Y., 2005. Paleozoic tectonic evolution of medio-europa from the example of the french massif central and massif armoricain. *Journal of Virtual Explorer*, 19, 1-26.
- Faure, M., Sommers, C., Melleton, J., Cocherie, A. & Lautout, O., 2008. The Léon Domain (French Massif Armoricain): a westward extension of the Mid-German Crystalline Rise? Structural and geochronological insights. *International Journal of Earth Sciences*, 99, 65-81.
- Gapais, D. & Cobbold, P.R., 1987. Slip system domains. 2. Kinematic aspects of fabric development in polycrystalline aggregates. *Tectonophysics*, 138, 289-309.
- Garreau, J., 1983. Géomorphologie structural en Bretagne péninsulaire. La région de Morlaix. *Norois*, 118, 195-212.
- Goré, B., Le Corre, C., 1987. Cinématique hercynienne du cisaillement nord-armoricain à la bordure du granite syntectonique de Saint Renan-Kersaint (Finistère). *Bulletin de la Société Géologique de France*, 8, 5, 811-819.
- Gumiaux, C., Judenherc, S., Brun, J.-P., Gapais, D., Granet, M. & Poupinet, G., 2004. Restoration of lithosphere-scale wrenching from integrated structural and tomographic data (Hercynian belt of western France). *Geology*, 32, 333-336.
- Kilb, D. & Rubin, A.M., 2002. Implications of diverse fault orientations imaged in relocated aftershocks of the Mount Lewis, ML 5.7, California, earthquake. *Journal of Geophysical Research*, 107, 2294-2311.
- Kim, Y.-S., Peacock, D.C.P. & Sanderson, D.J., 2003. Mesoscale strike-slip faults and damage zones at Marsalforn, Gozo Island, Malta. *Journal of Structural Geology*, 25, 793-812.
- Kim, Y.-S., Peacock, D.C.P. & Sanderson, D.J., 2004. Fault damage zones. *Journal of Structural Geology*, 26, 503-517.
- Lacombe, O., 2012. Do fault slip data inversions actually yield "paleostresses" that can be compared with contemporary stresses? A critical discussion. *Comptes Rendus Geoscience*, 344, 3-4, 159-173.
- Le Corre, C., Auvray, B., Balleve, M. & Robardet, M., 1991. Le Massif Armoricain. In: Piqué A. (éd.), *Les massifs anciens de France*, I. Sciences géologiques, Strasbourg, 44, 31-104.

- Matte, P., 2001. The Variscan collage and orogeny (480-290 Ma) and the tectonic definition of the Armorica microplate: a review. *Terra Nova*, 13, 2, 122-128.
- Maussen, K., 2010. Origin and characteristics of large-scale quartz bodies along the North-Armorican shear zone, Brittany, France. Master's thesis, Campus Library Arenberg KULeuven, 90.
- Michael, A.J., 1984. Determination of stress from slip data: faults and folds. *Journal of Geophysical Research*, 89, 517-526.
- Reches, Z., 1987. Determination of the tectonic stress tensor from slip along faults and that obey the Coulomb yield condition. *Tectonics*, 6, 846-861.
- Riedel, W., 1928. Zur Mechanik geologischer Brucherscheinungen. *Zentralblatt für Geologie und Paleontologie Abhandlung*, 13, 354-368.
- Scholz, C.H., 2003. *The mechanics of earthquakes and faulting*. Cambridge University Press, 471.
- Sintubin, M., van Noorden, M. & Berwouts, I., 2008. Late Devonian-Early Carboniferous contraction-dominated deformation in Central Armorica (Mont D'Arrée, Brittany, France) and its relationship with the closure of the Rheic Ocean. *Tectonophysics*, 461, 343-355.
- Srivastava, D.C., Lisle, R. J. & Vandycke, S., 1995. Shear zones as a new type of palaeostress indicator. *Journal of Structural Geology*, 17, 5, 663-676.
- Strachan, R.A., Treloar, P. J., Brown, M. & D'Lemos, R. S., 1989. Short Paper: Cadomian terrane tectonics and magmatism in the Armorican Massif. *Journal of the Geological Society, London*, 146, 423-426.
- Tchalenko, J.S., 1970. Similarities between shear zones of different magnitudes. *Geological Society of America Bulletin*, 81, 1625-1640.
- Van Noten, K., Muchez, P. & Sintubin, M., 2011. Stress-state evolution of the brittle upper crust during compressional tectonic inversion as defined by successive quartz vein-types (High-Ardenne slate belt, Germany). *Journal of the Geological Society, London*, 168, 2, 407-422.
- Van Noten, K., Van Baelen, H. & Sintubin, M., 2012. The complexity of 3D stress-state changes during compressional tectonic inversion at the onset of orogeny. *Geological Society, London, Special Publications*, 367, 51-69.
- Watts, M.J. & Williams, G. D., 1979. Fault rocks as indicators of progressive shear deformation in the Guingamp region, Brittany. *Journal of Structural Geology*, 1, 4, 323-332.
- Wilson, R.W., McCaffrey, K. J. W., Holdsworth, R. E., Imber, J., Jones, R. R., Welbon, A. I. & Roberts, D., 2006. Complex fault patterns, transtension and structural segmentation of the Lofoten Ridge, Norwegian Margin: using digital mapping to link onshore and offshore geology. *Tectonics*, 25, 1-28.

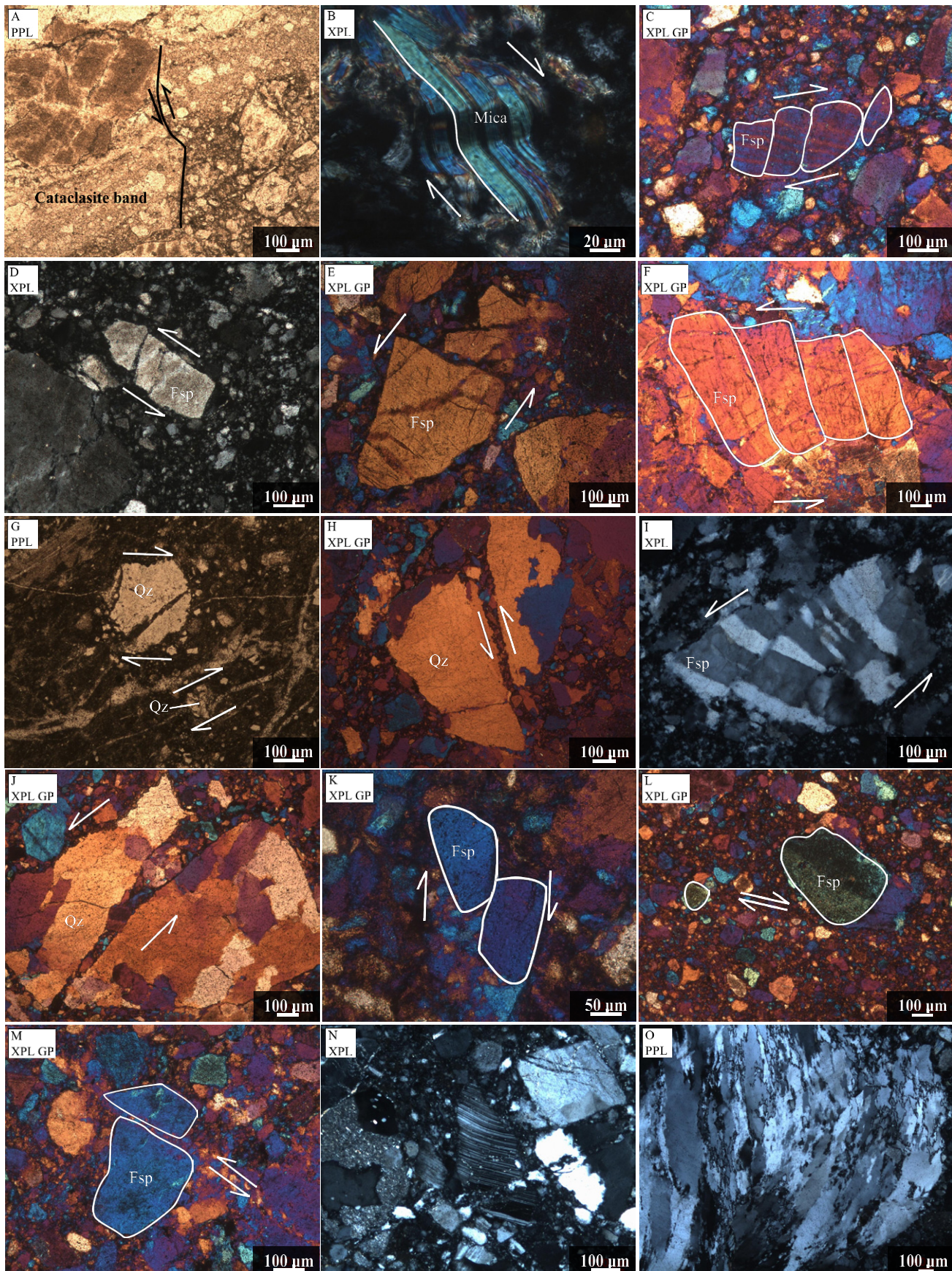


Plate 1. Petrography of the QCZ. Optical microscope photographs of (A) displaced cataclasite band, (C, D, E, F) bookshelf microfracturing, (G) δ -type winged mantled clast, (H, I, J, K, L, M) fragmented and displaced clasts. The observed structures indicate mixed sinistral and dextral displacements. (N) Bent twins in plagioclase. (O) Bulging and subgrain rotation dynamic recrystallisation in quartz. Fsp: feldspar, GP: gypsum plate, PPL: plane-polarised light, Qz: quartz, XPL: cross-polarised light.